Longitudinal Active Suspension Control in a Half-Car Model with Unsprang Masses

Automatic Control
Electronic Engineering for Intelligent Vehicles
University of Bologna

A.A. 2025-2026

Alessandro Briccoli, Cristian Cecchini, Mario Di Marino

February 15, 2026

Abstract

This report presents the modeling, design, and simulation of an active suspension control system aimed at improving ride comfort and handling performance in passenger vehicles. The study focuses on a half-car model that includes both front and rear suspension dynamics, allowing the analysis of vertical and pitch motion of the vehicle body. Unlike passive suspension systems, which rely solely on spring-damper elements, the active suspension system introduced here incorporates actuators capable of generating controlled forces to counteract road disturbances in real time.

To achieve the desired ride quality, a control strategy based on Proportional-Integral-Derivative (PID) controllers is developed. Additionally, a state estimation technique using a Kalman observer is incorporated to provide real-time estimates of the states, helping to adapt to acceleration and road profile in a faster and more effective way.

The performance of the control system is evaluated through simulations conducted in MATLAB/Simulink. Results show a significant reduction in body acceleration and pitch angle variation when compared to a passive suspension system, demonstrating the effectiveness of the proposed approach in enhancing ride comfort. This project perfectly demonstrates, once again, the massive importance of active control strategies in automotive suspension design.

Chapter 1

Introduction

1.1 Motivations

Suspension systems play a crucial role in ensuring vehicle stability, comfort, and safety. Traditional passive suspensions cannot adapt to changing road conditions, leading to undesired oscillations and reduced performance.

In this project, focus on active suspension control in the longitudinal direction (front and rear), which aims to reduce vertical oscillations and pitch movements when the vehicle passes over bumps or uneven surfaces. The goal is to design a control system that keeps the car body as steady as possible, improving both passenger comfort and vehicle handling.

The half-car model was chosen because it provides a good trade-off between model simplicity and dynamic realism and allows to study the impact of front and rear suspension forces on the vehicle behavior without dealing with the complexity of a full 3D model.

1.2 List of the symbols

Table 1.1: Symbol Table

Symbol	Description	Dimension
x	State vector	$\mathbb{R}^{12}$
u	Control input vector $[u_1\ u_2]^T$	$\mathbb{R}^2$
y	Measured output vector	$\mathbb{R}^5$
e	Control error vector	$\mathbb{R}^2$
d	Disturbance vector	$\mathbb{R}^6$
r	Reference vector $[r_z\ r_\theta]^T$	$\mathbb{R}^2$
ν	Sensor noise vector	$\mathbb{R}^5$
w	Exogenous input $w = \mathrm{col}(d, \nu, r)$	—
p_z	Vertical displacement of vehicle CoM	m
v_z	Vertical velocity of vehicle CoM	m/s
θ	Pitch angle of vehicle body	rad
$\dot{\theta}$	Pitch angular velocity	rad/s
h_{wf}, h_{wr}	Front and rear wheel vertical displacement	m
$\dot{h}_{wf}, \dot{h}_{wr}$	Front and rear wheel vertical velocity	m/s
θ_{gf}, θ_{gr}	Road pitch angle at front and rear axle	rad
z_{gf}, z_{gr}	Road vertical displacement at front and rear axle	m
u_1	Total vertical actuator force	N
u_2	Pitch moment component of actuator input	Nm
f_{af}, f_{ar}	Front and rear actuator forces	N
d_f, d_r	Distance from CoM to front and rear axle	m
h_{cg}	Height of vehicle center of mass	m
m	Sprung mass (vehicle body)	kg
m_{wf}, m_{wr}	Front and rear unsprung mass	kg
J	Pitch moment of inertia	$\mathrm{kg\,m^2}$
k_f, k_r	Front and rear suspension stiffness	N/m
β_f, β_r	Front and rear suspension damping	N s/m
k_{tf}, k_{tr}	Front and rear tire stiffness	N/m
s_1, s_3	Front and rear suspension deflection	m
s_2, s_4	Front and rear suspension velocity	m/s
f_{sf}, f_{sr}	Front and rear suspension forces	N
f_{wf}, f_{wr}	Front and rear wheel dynamics forces	N
f_{xf}, f_{xr}	Longitudinal forces at front and rear axle	N
F_x	Total longitudinal force $F_x = f_{xf} + f_{xr}$	N
f_2	Vertical acceleration of vehicle body	$\mathrm{m/s^2}$
f_4	Pitch angular acceleration	$\mathrm{rad/s^2}$
α_{gf}, α_{gr}	Road pitch angular acceleration (front, rear)	$\mathrm{rad/s^2}$
$\dot{z}_{gf}, \dot{z}_{gr}$	Road vertical velocity (front, rear)	m/s
y_x	Longitudinal accelerometer output	$\mathrm{m/s^2}$
y_z	Vertical accelerometer output	$\mathrm{m/s^2}$
y_θ	Gyroscope pitch-rate measurement	rad/s
y_f, y_r	Front and rear suspension sensors	m
$\nu_y, \nu_z, \nu_g, \nu_f, \nu_r$	Sensor noise components	—
r_z	Reference vertical position	m
r_θ	Reference pitch angle	rad
g	Gravitational acceleration	$\mathrm{m/s^2}$
γ_f	Anti-Dive suspension inclination	—
γ_r	Anti-Squat suspension inclination	—

1.2.1 Dynamic Model

The considered vehicle model is a nonlinear longitudinal half-car representation equipped with two independently actuated suspensions. The model captures the vertical and pitch dynamics of the sprung mass, as well as the vertical dynamics of the front and rear unsprung masses. Tire compliance is explicitly included through linear tire stiffness, allowing the interaction between the wheels and the road profile to be accurately represented.

The sprung mass is assumed to be a rigid body with two degrees of freedom: vertical translation and pitch rotation. Each unsprung mass is modeled as a single vertical degree of freedom. Road excitations are treated as external inputs acting at the tire–road contact points and are not included as dynamic states.

State vector

The system state vector is defined as:

$$x = \begin{bmatrix} z_s & \dot{z}_s & \theta & \dot{\theta} & z_{wf} & \dot{z}_{wf} & z_{wr} & \dot{z}_{wr} \end{bmatrix}^T \in \mathbb{R}^8 \tag{1.1}$$

where z_s and $\dot{z}_s$ denote the vertical displacement and velocity of the sprung mass center of mass, θ and $\dot{\theta}$ are the pitch angle and pitch rate, while z_{wf}, z_{wr} and their time derivatives describe the vertical motion of the front and rear unsprung masses.

Control inputs

The active suspension system is driven by two control inputs:

$$u = \begin{bmatrix} u_1 \\ u_2 \end{bmatrix} \tag{1.2}$$

where u_1 represents the total vertical force applied to the sprung mass, and u_2 is the pitching moment about the center of mass. The corresponding actuator forces at the front and rear suspensions are obtained through the static force distribution:

$$f_{af} = \frac{d_r u_1 + u_2}{d_f + d_r}, \tag{1.3}$$

$$f_{ar} = \frac{d_f u_1 - u_2}{d_f + d_r}, \tag{1.4}$$

with d_f and d_r denoting the distances from the center of mass to the front and rear axles, respectively.

Suspension kinematics

The suspension deflections and relative velocities are given by:

$$s_1 = z_s + d_f \sin\theta - z_{wf}, \qquad s_3 = z_s - d_r \sin\theta - z_{wr}, \tag{1.5}$$

$$s_2 = \dot{z}_s + d_f \dot{\theta} \cos\theta - \dot{z}_{wf}, \qquad s_4 = \dot{z}_s - d_r \dot{\theta} \cos\theta - \dot{z}_{wr}. \tag{1.6}$$

These expressions account for both the translational motion of the sprung mass and the geometric contribution due to pitch rotation.

Suspension and tire forces

The suspension forces are modeled as linear spring–damper elements:

$$f_{sf} = -k_f s_1 - \beta_f s_2, \tag{1.7}$$

$$f_{sr} = -k_r s_3 - \beta_r s_4, \tag{1.8}$$

where k_f, k_r and β_f, β_r are the stiffness and damping coefficients of the front and rear suspensions.

The tire–road interaction is described using linear tire stiffness:

$$f_{tf} = k_{tf}(z_{rf} - z_{wf}), \tag{1.9}$$

$$f_{tr} = k_{tr}(z_{rr} - z_{wr}), \tag{1.10}$$

with z_{rf} and z_{rr} denoting the vertical road displacements at the front and rear contact points.

Sprung mass dynamics

The vertical acceleration of the sprung mass follows from Newton's second law:

$$\ddot{z}_s = -g + \frac{1}{m}\left(f_{sf} + f_{sr} + f_{af} + f_{ar}\right). \tag{1.11}$$

The pitch dynamics about the center of mass are governed by:

$$\ddot{\theta} = \frac{1}{J}\left(d_f(f_{sf} + f_{af}) - d_r(f_{sr} + f_{ar}) + h_{cg}F_x\right), \tag{1.12}$$

where J is the pitch moment of inertia, h_{cg} is the height of the center of mass, and

$$F_x = F_{xf} + F_{xr} \tag{1.13}$$

is the resultant longitudinal force acting on the vehicle. This term accounts for the coupling between longitudinal forces and pitch dynamics through load transfer effects.

Unsprung mass dynamics

The vertical dynamics of the front and rear unsprung masses are given by:

$$\ddot{z}_{wf} = \frac{1}{m_{wf}} \left(f_{tf} - f_{sf} - f_{af} - m_{wf} g \right), \tag{1.14}$$

$$\ddot{z}_{wr} = \frac{1}{m_{wr}} \left(f_{tr} - f_{sr} - f_{ar} - m_{wr} g \right). \tag{1.15}$$

State-space representation

Collecting all terms, the nonlinear vehicle dynamics can be written in first-order state-space form as:

$$\dot{x} = f(x, u, w, road), \tag{1.16}$$

where w represents external longitudinal force disturbances and $road$ collects the road profile inputs at the wheel contact points.

This formulation provides a complete nonlinear description of the vertical and pitch dynamics of the vehicle, forming the basis for linearization, controller synthesis, and observer design.

1.2.2 Sensor Model

The control architecture relies on a set of onboard sensors that provide real-time measurements of the vehicle vertical and pitch dynamics. The selected sensor suite is designed to ensure observability of the nonlinear half-car model and to provide sufficient information for feedback control in the presence of road disturbances and measurement noise.

All sensor measurements are assumed to be affected by additive noise and are expressed in the vehicle body-fixed reference frame.

Measurement Vector

The complete measurement vector is defined as:

$$y = \begin{bmatrix} y_y \\ y_z \\ y_g \\ y_f \\ y_r \end{bmatrix} = \begin{bmatrix} \sin(\theta)(f_2 + g) + \cos(\theta)\frac{F_x}{m} \\ \cos(\theta)(f_2 + g) - \sin(\theta)\frac{F_x}{m} \\ \dot{\theta} \\ s_1 \\ s_3 \end{bmatrix} + \begin{bmatrix} \nu_y \\ \nu_z \\ \nu_g \\ \nu_f \\ \nu_r \end{bmatrix}. \tag{1.17}$$

This vector includes measurements from two accelerometers, one gyroscope, and two suspension displacement sensors.

Accelerometer Model

The first two outputs y_y and y_z represent the longitudinal and vertical accelerations measured in the body-fixed reference frame. These signals are obtained from MEMS accelerometers mounted near the vehicle center of mass.

The accelerometer outputs are nonlinear functions of the vehicle dynamics and include both inertial and gravitational contributions. The term $f_2 + g$ corresponds to the absolute vertical acceleration of the sprung mass, while F_x/m represents the longitudinal acceleration induced by external forces.

The trigonometric terms $\sin(\theta)$ and $\cos(\theta)$ account for the projection of the acceleration vector onto the body-fixed axes due to the pitch angle, resulting in an intrinsic coupling between vertical and pitch dynamics.

A typical automotive-grade device is the **STMicroelectronics LIS3DH**, providing 12-bit resolution and low noise density.

Gyroscope Model

The third measurement y_g corresponds to the pitch angular rate:

$$y_g = \dot{\theta} + \nu_g. \tag{1.18}$$

This signal is provided by a gyroscope rigidly attached to the vehicle body and delivers high-bandwidth information essential for pitch stabilization and transient response improvement.

Figure 1.1: MEMS accelerometer LIS3DH

A representative sensor is the **Bosch BMI160**, integrating accelerometer and gyroscope within a compact IMU package.

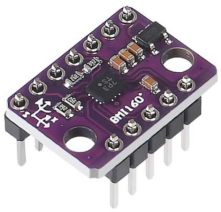

Figure 1.2: Bosch BMI160 IMU

Suspension Deflection Sensors

The last two measurements y_f and y_r correspond to the front and rear suspension deflections:

$$y_f = s_1 + \nu_f, \qquad y_r = s_3 + \nu_r. \tag{1.19}$$

The deflections are defined as:

$$s_1 = (z_s + d_f \sin\theta) - z_{wf}, \tag{1.20}$$

$$s_3 = (z_s - d_r \sin\theta) - z_{wr}, \tag{1.21}$$

and represent the relative displacement between the sprung mass and the unsprung masses. These measurements provide direct information on road excitation and wheel–body interaction.

Linear potentiometers such as the **SLS190** are assumed.

Figure 1.3: Linear suspension potentiometer

Noise Modeling

All sensor measurements are affected by additive noise:

$$\nu = \begin{bmatrix} \nu_y & \nu_z & \nu_g & \nu_f & \nu_r \end{bmatrix}^T. \tag{1.22}$$

Noise components are modeled as zero-mean Gaussian processes with variances derived from typical automotive sensor specifications. Accelerometers and gyroscopes include white noise and bias drift, while suspension sensors are mainly affected by quantization and thermal noise.

1.3 Performance Variables and Control Objectives

To evaluate the effectiveness of the active suspension system and to formulate the optimization problem (e.g., for optimal control or performance monitoring), a specific performance output vector $z \in \mathbb{R}^6$ is defined. Unlike the measured output vector y, which depends on available sensors, the vector z contains the physical variables that strictly define the ride quality and the mechanical constraints of the vehicle.

The performance vector is constructed as a function of the state vector x, the vehicle parameters p, and the reference vector r:

$$z = g(x, p, r) \tag{1.23}$$

1.3.1 State and Reference Definitions

Consistent with the system model, the relevant state variables for performance monitoring are:

- $z_s = x_1$: Vertical position of the sprung mass CoM (Heave).
- $\dot{z}_s = x_2$: Vertical velocity of the sprung mass (Heave velocity).

- $\theta = x_3$: Pitch angle.
- $\dot{\theta} = x_4$: Pitch rate.
- $z_{wf} = x_5$, $z_{wr} = x_7$: Vertical positions of the front and rear unsprung masses (wheels).

The reference vector $r \in \mathbb{R}^2$ defines the target tracking trajectory:

$$r = \begin{bmatrix} r_z \\ r_\theta \end{bmatrix} \tag{1.24}$$

where r_z is the desired heave position (typically the static equilibrium height) and r_θ is the desired pitch angle (typically zero to maintain a flat chassis).

1.3.2 Suspension Deflections

The suspension deflections (or working spaces), denoted as s_f and s_r, represent the relative compression between the vehicle body and the wheels. To account for the geometric coupling induced by significant pitch rotations, these are calculated using the exact kinematic relationships:

$$s_f = (z_s + d_f \sin\theta) - z_{wf} \tag{1.25}$$
$$s_r = (z_s - d_r \sin\theta) - z_{wr} \tag{1.26}$$

Here, d_f and d_r represent the longitudinal distances from the center of mass to the front and rear axles, respectively. The term $\sin\theta$ ensures that the vertical displacement of the suspension mounting points is correctly mapped even for non-small pitch angles.

1.3.3 Performance Vector Definition

The resulting performance vector z is composed of six elements, each addressing a specific control objective:

$$z = \begin{bmatrix} z_1 \\ z_2 \\ z_3 \\ z_4 \\ z_5 \\ z_6 \end{bmatrix} = \begin{bmatrix} z_s - r_z \\ \theta - r_\theta \\ \dot{\theta} \\ s_f \\ s_r \\ \dot{z}_s \end{bmatrix} \tag{1.27}$$

Physical Interpretation

The components of z are selected to monitor and minimize the following behaviors:

1. **Heave Regulation Error (z_1):** Ensures the vehicle maintains the desired ride height r_z despite external loads or disturbances.

2. **Pitch Regulation Error (z_2):** Critical for the "Magic Carpet" effect; minimizing this term prevents the vehicle from squatting or diving during acceleration and braking.

3. **Pitch Damping (z_3):** Minimizing the pitch rate $\dot{\theta}$ reduces rotational oscillations, improving passenger comfort.

4. **Suspension Travel (z_4, z_5):** Monitoring s_f and s_r is essential to keep the suspension excursions within the mechanical structural limits (avoiding bump-stop impacts).

5. **Heave Damping (z_6):** Minimizing the vertical velocity $\dot{z}_s$ dissipates the energy induced by road irregularities, reducing the "pumping" effect of the chassis.

This definition of z allows for a comprehensive assessment of the trade-off between ride comfort (minimized accelerations and velocities) and handling/safety (bounded suspension travel and accurate attitude tracking).

Observability Considerations

The selected sensor configuration ensures observability of the states relevant for control. Accelerometer and gyroscope measurements capture translational and rotational dynamics, while suspension deflection sensors resolve wheel–body interaction and road-induced disturbances, enabling reliable state estimation through standard observers.

1.3.4 System Linearization

To facilitate the control design of the longitudinal half-car model equipped with active front and rear suspension systems, the initial step involves the linearization of the nonlinear system dynamics. This process is performed by identifying appropriate steady-state operating points (x^*, y^*, w^*), which characterize representative conditions under which the vehicle is expected to operate. Linearizing the system around these equilibrium points enables the derivation of a time-invariant linear approximation of the vehicle dynamics, thereby simplifying the synthesis and analysis of control strategies.

Linearization Around the Operating Point

Consider the nonlinear system model:

$$\begin{aligned} \dot{x} &= f(x, u, w), \quad x(t_0) = x_0 \\ y &= h(x, u, w) \\ e &= h_e(x, u, w) \end{aligned} \tag{1.28}$$

The steady-state operating points $(x^\star, u^\star, w^\star)$ is called *equilibrium triplet* if satisfies the condition:

$$f(x^\star, u^\star, w^\star) = 0 \tag{1.29}$$

and defines the equilibrium output and error as:

$$y^\star := h(x^\star, u^\star, w^\star), \quad e^\star := h_e(x^\star, u^\star, w^\star) \tag{1.30}$$

The variations around the equilibrium point are defined as:

$$\begin{aligned} \tilde{x} &:= x - x^\star \\ \tilde{y} &:= y - y^\star \\ \tilde{e} &:= e - e^\star \\ \tilde{u} &:= u - u^\star \\ \tilde{w} &:= w - w^\star \end{aligned} \tag{1.31}$$

Using the fact that $\dot{x}^\star = 0$, the dynamics of the variations are:

$$\begin{aligned} \dot{\tilde{x}} &= f(x^\star + \tilde{x}, u^\star + \tilde{u}, w^\star + \tilde{w}), \quad \tilde{x}(t_0) = x_0 - x^\star \\ \tilde{y} &= h(x^\star + \tilde{x}, u^\star + \tilde{u}, w^\star + \tilde{w}) \\ \tilde{e} &= h_e(x^\star + \tilde{x}, u^\star + \tilde{u}, w^\star + \tilde{w}) \end{aligned} \tag{1.32}$$

To obtain a tractable model for controller synthesis, a first-order Taylor expansion is applied around the equilibrium point. The resulting Jacobian ma-

trices are defined as:

$$
\begin{aligned}
A &:= \left.\frac{\partial f(x,u,w)}{\partial x}\right|_{\substack{x=x^\star\\u=u^\star\\w=w^\star}} \qquad B_1 := \left.\frac{\partial f(x,u,w)}{\partial u}\right|_{\substack{x=x^\star\\u=u^\star\\w=w^\star}} \qquad B_2 := \left.\frac{\partial f(x,u,w)}{\partial w}\right|_{\substack{x=x^\star\\u=u^\star\\w=w^\star}} \\
C &:= \left.\frac{\partial h(x,u,w)}{\partial x}\right|_{\substack{x=x^\star\\u=u^\star\\w=w^\star}} \qquad D_1 := \left.\frac{\partial h(x,u,w)}{\partial u}\right|_{\substack{x=x^\star\\u=u^\star\\w=w^\star}} \qquad D_2 := \left.\frac{\partial h(x,u,w)}{\partial w}\right|_{\substack{x=x^\star\\u=u^\star\\w=w^\star}} \\
C_e &:= \left.\frac{\partial h_e(x,u,w)}{\partial x}\right|_{\substack{x=x^\star\\u=u^\star\\w=w^\star}} \qquad D_{e1} := \left.\frac{\partial h_e(x,u,w)}{\partial u}\right|_{\substack{x=x^\star\\u=u^\star\\w=w^\star}} \qquad D_{e2} := \left.\frac{\partial h_e(x,u,w)}{\partial w}\right|_{\substack{x=x^\star\\u=u^\star\\w=w^\star}}
\end{aligned}
\tag{1.33}
$$

Neglecting second-order terms, the linearized system becomes the so-called *design model*:

$$
\begin{cases}
\dot{\tilde{x}} = A\tilde{x} + B_1\tilde{u} + B_2\tilde{w}, \quad \tilde{x}(t_0) = x_0 - x^\star \\
\tilde{y} = C\tilde{x} + D_1\tilde{u} + D_2\tilde{w} \\
\tilde{e} = C_e\tilde{x} + D_{e1}\tilde{u} + D_{e2}\tilde{w}
\end{cases}
\tag{1.34}
$$

This Linear Time-Invariant (LTI) approximation of the nonlinear model is valid in a neighborhood of the equilibrium point, enabling efficient analysis and controller design under small perturbations.

Matrix calculus

For the matrix calculation, the procedure described in equations (1.33) was followed. By substituting the equilibrium triplet given in (1.29), obtaining the following matrices:

$$
A = \begin{bmatrix}
0 & 1 & 0 & 0 & 0 & 0 & 0 & 0 & 0 & 0 & 0 & 0 \\
-\frac{k_f+k_r}{m} & -\frac{\beta_f+\beta_r}{m} & -\frac{d_f k_f - d_r k_r}{m} & -\frac{\beta_f d_f - \beta_r d_r}{m} & \frac{k_f}{m} & \frac{\beta_f}{m} & \frac{k_r}{m} & \frac{\beta_r}{m} & 0 & 0 & 0 & 0 \\
0 & 0 & 0 & 1 & 0 & 0 & 0 & 0 & 0 & 0 & 0 & 0 \\
-\frac{d_f k_f - d_r k_r}{J} & -\frac{\beta_f d_f - \beta_r d_r}{J} & -\frac{k_f d_f^2 + k_r d_r^2}{J} & -\frac{\beta_f d_f^2 + \beta_r d_r^2}{J} & \frac{d_f k_f}{J} & \frac{\beta_f d_f}{J} & -\frac{d_r k_r}{J} & -\frac{\beta_r d_r}{J} & 0 & 0 & 0 & 0 \\
0 & 0 & 0 & 0 & 0 & 1 & 0 & 0 & 0 & 0 & 0 & 0 \\
\frac{k_f}{m_{wf}} & \frac{\beta_f}{m_{wf}} & \frac{d_f k_f}{m_{wf}} & \frac{\beta_f d_f}{m_{wf}} & -\frac{k_f+k_{tf}}{m_{wf}} & -\frac{\beta_f}{m_{wf}} & 0 & 0 & 0 & 0 & \frac{k_{tf}}{m_{wf}} & 0 \\
0 & 0 & 0 & 0 & 0 & 0 & 0 & 1 & 0 & 0 & 0 & 0 \\
\frac{k_r}{m_{wr}} & \frac{\beta_r}{m_{wr}} & -\frac{d_r k_r}{m_{wr}} & -\frac{\beta_r d_r}{m_{wr}} & 0 & 0 & -\frac{k_r+k_{tr}}{m_{wr}} & -\frac{\beta_r}{m_{wr}} & 0 & 0 & 0 & \frac{k_{tr}}{m_{wr}} \\
0 & 0 & 0 & 0 & 0 & 0 & 0 & 0 & 0 & 0 & 0 & 0 \\
0 & 0 & 0 & 0 & 0 & 0 & 0 & 0 & 0 & 0 & 0 & 0 \\
0 & 0 & 0 & 0 & 0 & 0 & 0 & 0 & 0 & 0 & 0 & 0 \\
0 & 0 & 0 & 0 & 0 & 0 & 0 & 0 & 0 & 0 & 0 & 0
\end{bmatrix}
\tag{1.35}
$$

$$B_1 = \begin{bmatrix} 0 & 0 \\ \frac{1}{m} & 0 \\ 0 & 0 \\ 0 & \frac{1}{J} \\ 0 & 0 \\ -\frac{d_r}{m_{wf}(d_f+d_r)} & -\frac{1}{m_{wf}(d_f+d_r)} \\ 0 & 0 \\ -\frac{d_f}{m_{wr}(d_f+d_r)} & \frac{1}{m_{wr}(d_f+d_r)} \\ 0 & 0 \\ 0 & 0 \\ 0 & 0 \\ 0 & 0 \end{bmatrix} \tag{1.36}$$

$$B_2 = \begin{bmatrix} 0 & 0 & 0 & 0 & 0 & 0 \\ 0 & 0 & 0 & 0 & 0 & 0 \\ 0 & 0 & 0 & 0 & 0 & 0 \\ 0 & 0 & 0 & 0 & \frac{h_{cg}}{J} & \frac{h_{cg}}{J} \\ 0 & 0 & 0 & 0 & 0 & 0 \\ 0 & 0 & 0 & 0 & 0 & 0 \\ 0 & 0 & 0 & 0 & 0 & 0 \\ 0 & 0 & 0 & 0 & 0 & 0 \\ 0 & 0 & 1 & 0 & 0 & 0 \\ 0 & 0 & 0 & 1 & 0 & 0 \\ 1 & 0 & 0 & 0 & 0 & 0 \\ 0 & 1 & 0 & 0 & 0 & 0 \end{bmatrix} \tag{1.37}$$

$$C = \begin{bmatrix} 0 & 0 & \frac{0.350357(k_f+k_r)}{m} & 0 & 0 & 0 & 0 & 0 & 0 & 0 & 0 \\ -\frac{k_f+k_r}{m} & -\frac{\beta_f+\beta_r}{m} & -\frac{d_f k_f - d_r k_r}{m} & -\frac{\beta_f d_f - \beta_r d_r}{m} & \frac{k_f}{m} & \frac{\beta_f}{m} & \frac{k_r}{m} & \frac{\beta_r}{m} & 0 & 0 & 0 & 0 \\ 0 & 0 & 0 & 1 & 0 & 0 & 0 & 0 & 0 & 0 & 0 & 0 \\ 1 & 0 & d_f & 0 & -1 & 0 & 0 & 0 & 0 & 0 & 0 & 0 \\ 1 & 0 & -d_r & 0 & 0 & 0 & -1 & 0 & 0 & 0 & 0 & 0 \end{bmatrix} \tag{1.38}$$

$$D_1 = \begin{bmatrix} 0 & 0 \\ \frac{1}{m} & 0 \\ 0 & 0 \\ 0 & 0 \\ 0 & 0 \end{bmatrix} \tag{1.39}$$

$$D_2 = \begin{bmatrix} 0 & 0 & 0 & 0 & \frac{1}{m} & \frac{1}{m} & 1 & 0 & 0 & 0 & 0 & 0 & 0 \\ 0 & 0 & 0 & 0 & 0 & 0 & 0 & 1 & 0 & 0 & 0 & 0 & 0 \\ 0 & 0 & 0 & 0 & 0 & 0 & 0 & 0 & 1 & 0 & 0 & 0 & 0 \\ 0 & 0 & 0 & 0 & 0 & 0 & 0 & 0 & 0 & 1 & 0 & 0 & 0 \\ 0 & 0 & 0 & 0 & 0 & 0 & 0 & 0 & 0 & 0 & 1 & 0 & 0 \end{bmatrix} \tag{1.40}$$

$$D_{e1} = \begin{bmatrix} 0 & 0 \\ 0 & 0 \end{bmatrix} \tag{1.41}$$

$$D_{e2} = \begin{bmatrix} 0 & 0 & 0 & 0 & 0 & 0 & 0 & 0 & 0 & \frac{d_r}{d_f + d_r} & \frac{d_f}{d_f + d_r} & -1 & 0 \\ 0 & 0 & 0 & 0 & 0 & 0 & 0 & 0 & 0 & 0 & 0 & 0 & -1 \end{bmatrix} \tag{1.42}$$

$$C_e = \begin{bmatrix} 1 & 0 & 0 & 0 & -\frac{d_r}{d_f + d_r} & 0 & -\frac{d_f}{d_f + d_r} & 0 & 0 & 0 & 0 & 0 \\ 0 & 0 & 1 & 0 & 0 & 0 & 0 & 0 & 0 & 0 & 0 & 0 \end{bmatrix} \tag{1.43}$$

Numerical Matrices To calculate the numerical values of the matrices, the parameters were replaced with the values of the vehicle chosen for this study: All parameters used to find the numeric matrices are based on the Tesla Model S, a car suitable for this type of active suspensions and with same suspension paramethers on front and rear axle, this simplifies slighlty our model:

Figure 1.4: Rolls-Royce Ghost 6.7 V12

Symbol	Description	Value	Unit
m	Total mass of the vehicle	2550	kg
g	Gravitational acceleration	9.81	$\mathrm{m/s^2}$
h_{cg}	Height of center of gravity	0.60	m
d_f	Front axle distance from CoM	1.65	m
d_r	Rear axle distance from CoM	1.65	m
L	Wheelbase	3.30	m
J	Pitch moment of inertia	4080	$\mathrm{kg{\cdot}m^2}$
k_f	Front suspension stiffness	35000	N/m
k_r	Rear suspension stiffness	32000	N/m
β_f	Front damping coefficient	4200	N·s/m
β_r	Rear damping coefficient	4200	N·s/m
m_{wf}	Front unsprung mass	48	kg
m_{wr}	Rear unsprung mass	48	kg
k_{tf}	Front tire stiffness	270000	N/m
k_{tr}	Rear tire stiffness	270000	N/m
ℓ_0	Static suspension height	0.55	m

Table 1.2: Dynamic model parameters of a Rolls-Royce vehicle (Half-Car Model)

$$A = 10^3 \begin{bmatrix} 0 & 0.0010 & 0 & 0 & 0 & 0 & 0 & 0 & 0 & 0 & 0 & 0 \\ -0.0280 & -0.0036 & -0.0009 & 0.0009 & 0.0164 & 0.0018 & 0.0116 & 0.0018 & 0 & 0 & 0 & 0 \\ 0 & 0 & 0 & 0.0010 & 0 & 0 & 0 & 0 & 0 & 0 & 0 & 0 \\ -0.0004 & 0.0004 & -0.0340 & -0.0046 & 0.0105 & 0.0012 & -0.0101 & -0.0016 & 0 & 0 & 0 & 0 \\ 0 & 0 & 0 & 0 & 0 & 0.0010 & 0 & 0 & 0 & 0 & 0 & 0 \\ 0.9111 & 0.1000 & 1.2756 & 0.1400 & -7.1333 & -0.1000 & 0 & 0 & 0 & 0 & 6.2222 & 0 \\ 0 & 0 & 0 & 0 & 0 & 0 & 0 & 0.0010 & 0 & 0 & 0 & 0 \\ 0.6444 & 0.1000 & -1.2244 & -0.1900 & 0 & 0 & -6.8667 & -0.1000 & 0 & 0 & 0 & 6.2222 \\ 0 & 0 & 0 & 0 & 0 & 0 & 0 & 0 & 0 & 0 & 0 & 0 \\ 0 & 0 & 0 & 0 & 0 & 0 & 0 & 0 & 0 & 0 & 0 & 0 \\ 0 & 0 & 0 & 0 & 0 & 0 & 0 & 0 & 0 & 0 & 0 & 0 \\ 0 & 0 & 0 & 0 & 0 & 0 & 0 & 0 & 0 & 0 & 0 & 0 \end{bmatrix} \tag{1.44}$$

$$B_1 = \begin{bmatrix} 0 & 0 \\ 0.000921659 & 0 \\ 0 & 0 \\ 0 & 0.000205339 \\ 0 & 0 \\ 0 & 0 \\ 0 & 0 \\ 0 & 0 \end{bmatrix} \tag{1.45}$$

$$B_2 = \begin{bmatrix} 0 & 0 & 0 & 0 & 0 \\ -1 & 0 & 0 & 0 & 0 \\ 0 & 0 & 0 & 0 & 0 \\ 0 & 0 & 0 & 0.0000662428 & 0.0000662428 \\ 0 & 0 & 0 & 0 & 0 \\ 0 & 0 & 0 & 0 & 0 \\ 0 & 1 & 0 & 0 & 0 \\ 0 & 0 & 1 & 0 & 0 \end{bmatrix} \tag{1.46}$$

$$C = \begin{bmatrix} 0 & 0 & 9.81 & 0 & 0 & 0 & 0 & 0 \\ -55.2995 & -3.68664 & 6.52535 & 0.435023 & 37.659 & -44.1843 & 2.5106 & -2.94562 \\ 0 & 0 & 0 & 1 & 0 & 0 & 0 & 0 \\ 1 & 0 & 1.362 & 0 & -1.362 & 0 & 0 & 0 \\ 1 & 0 & -1.598 & 0 & 0 & 1.598 & 0 & 0 \end{bmatrix} \tag{1.47}$$

$$D_1 = \begin{bmatrix} 0 & 0 \\ 0.000921659 & 0 \\ 0 & 0 \\ 0 & 0 \\ 0 & 0 \end{bmatrix} \tag{1.48}$$

$$D_2 = \begin{bmatrix} 0 & 0 & 0 & 0.000921659 & 0.000921659 & 1 & 0 & 0 & 0 & 0 & 0 & 0 \\ 0 & 0 & 0 & 0 & 0 & 0 & 1 & 0 & 0 & 0 & 0 & 0 \\ 0 & 0 & 0 & 0 & 0 & 0 & 0 & 1 & 0 & 0 & 0 & 0 \\ 0 & 0 & 0 & 0 & 0 & 0 & 0 & 0 & 1 & 0 & 0 & 0 \\ 0 & 0 & 0 & 0 & 0 & 0 & 0 & 0 & 0 & 1 & 0 & 0 \end{bmatrix} \tag{1.49}$$

$$C_e = \begin{bmatrix} 1 & 0 & 0 & 0 & -0.735296 & 0.735296 & 0 & 0 \\ 0 & 0 & 1 & 0 & 0 & 0 & 0 & 0 \end{bmatrix} \tag{1.50}$$

$$D_{e2} = \begin{bmatrix} 0 & 0 & 0 & 0 & 0 & 0 & 0 & 0 & 0.539865 & 0.460135 & -1 & 0 \\ 0 & 0 & 0 & 0.000093951 & 0.000093951 & 0.101937 & 0 & 0 & 0 & 0 & 0 & -1 \end{bmatrix} \tag{1.51}$$

1.3.5 Linear Model Analysis

To support the development of an effective suspension controller and gain insight into the vehicle's dynamic behavior, we examine a linearized model of a half-car system. This analysis is performed around a nominal equilibrium point, where the vehicle is at rest with zero pitch angle and no vertical or angular velocities. The focus is on the open-loop dynamics of the vehicle body, excluding actuator behavior and wheel compliance.

The model captures the essential vertical (heave) and angular (pitch) motions of the chassis. The state vector is defined as:

$$x = \begin{bmatrix} z - z_0 \\ \dot{z} \\ \theta \\ \dot{\theta} \end{bmatrix} \tag{1.52}$$

where z_0 is the vertical position of the center of mass at static equilibrium, and θ denotes the pitch angle of the chassis. The state-space representation of the system is given by:

$$\dot{x} = A_{\text{int}} x \tag{1.53}$$

Analysis of this reduced 4x4 matrix will be performed, ignoring the 4 exogenous states, the reason behind this is explained later in chapter 1.4 (Reachability) **todo: ricalcolare**

$$A_{\text{int}} = \begin{bmatrix} 0 & 1 & 0 & 0 \\ -55.2995 & -3.68664 & 6.52535 & 0.435023 \\ 0 & 0 & 0 & 1 \\ 1.4538 & 0.0969199 & -27.158 & -1.81053 \end{bmatrix} \tag{1.54}$$

This matrix characterizes the coupled dynamics of the system, with off-diagonal elements indicating interaction between vertical and angular motions. Such coupling arises naturally in a physical half-car system, where vertical displacements can induce pitching, and vice versa.

1.3.6 Open-Loop Dynamics

To evaluate the system's stability and transient behavior, is necessary to calculate the eigenvalues of the matrix A_{int} by solving the characteristic equation:

$$\det(A_{\text{int}} - \lambda I) = 0 \tag{1.55}$$

The resulting eigenvalues are:

todo: ricalcolare

$$\lambda_{1,2} = -1.55 \pm j6.28, \quad \lambda_{3,4} = -2.47 \pm j5.10 \tag{1.56}$$

The eigenvalues form two pairs of complex conjugates, each with negative real parts, indicating that the system is asymptotically stable in open loop. These pairs represent distinct oscillatory modes characterized by different damping and frequency properties:

- The eigenvalues $\lambda_{1,2}$ correspond to a lightly damped oscillatory mode with a higher frequency.
- The eigenvalues $\lambda_{3,4}$ correspond to a more heavily damped mode with a lower oscillation frequency.

Due to the coupling present in A_{int}, these modes represent mixed heave-pitch dynamics rather than purely vertical or angular motions. This hybrid behavior implies that any disturbance in one degree of freedom can propagate to the other, necessitating a control strategy that accounts for this interaction.

The system's open-loop stability ensures that disturbances decay over time, but the oscillatory nature of the transients may degrade ride comfort and vehicle handling. Therefore, active suspension control is warranted to suppress these vibrations more rapidly, reduce settling time, and improve overall vehicle performance.

In summary, the linearized model described by A_{int} reveals a stable but dynamically coupled system with oscillatory characteristics. These insights are essential for the design of coordinated control strategies that enhance both ride quality and dynamic response.

1.4 Control

Reachability

In this section, a reachability analysis is carried out to determine which parts of the system's state space can be influenced by the control input. Starting from the linearized state-space system:

$$\dot{\tilde{x}} = A\tilde{x} + B_1\tilde{u} \tag{1.57}$$

we aim to identify which states can be driven from the origin to a desired position through the control input $\tilde{u}$. The reachability matrix is defined as:

$$\mathcal{R} = \begin{bmatrix} B_1 & AB_1 & A^2B_1 & \dots & A^{n-1}B_1 \end{bmatrix} \tag{1.58}$$

A linear time-invariant system is said to be **fully reachable** (or controllable from the origin) if the rank of $\mathcal{R}$ is equal to n, the number of state variables. In such a case, it is possible to design a state feedback controller that places all eigenvalues of the closed-loop system arbitrarily.

In our case, the system has $n = 8$ state variables. These include both the vehicle body dynamics (vertical position and velocity, pitch angle and rate) and road-related exogenous components (front and rear road pitch angles and their derivatives). The control input $\tilde{u} \in \mathbb{R}^2$ acts through actuators located at the front and rear suspensions, influencing primarily the body dynamics of the vehicle.

However, the states related to the road excitation are not directly controllable. As such, only a subset of the full state vector can be affected by $\tilde{u}$. Upon computation of the reachability matrix $\mathcal{R}$ using the specific system matrices A and B_1, we obtain:
todo: ricalcolare

```
R = ctrb(A, B1);
rank_R = rank(R);
```

$$\text{rank}(\mathcal{R}) = 4 < 8 \tag{1.59}$$

This indicates that the system is **not fully reachable**. Only the four states corresponding to the internal dynamics of the vehicle body are reachable, while the remaining four states — associated with the road profile — are uncontrollable and must be treated as external disturbances. Consequently, control strategies such as state feedback and optimal control (e.g., LQR) can only be designed for the reachable subspace.

Reduced Reachability Analysis

In the present model, the state vector $\tilde{x} \in \mathbb{R}^8$ includes eight components. However, the last four states represent environmental or road-related variables (e.g., road profile curvature), which evolve independently of the control input $\tilde{u}$. These are known as **exogenous states** and are not directly controllable.

Therefore, reachability analysis is performed only on the first four states, which represent the internal vehicle dynamics and are influenced by control inputs. Let A_{int} and $B_{1,\text{int}}$ be the upper-left 4×4 and 4×2 blocks of matrices A and B_1:

todo: ricalcolare:

$$A_{\text{int}} = \begin{bmatrix} 0 & 1 & 0 & 0 \\ -55.2995 & -3.68664 & 6.52535 & 0.435023 \\ 0 & 0 & 0 & 1 \\ 1.4538 & 0.0969199 & -27.158 & -1.81053 \end{bmatrix} \tag{1.60}$$

$$B_{1,\text{int}} = \begin{bmatrix} 0 & 0 \\ 0.000921659 & 0 \\ 0 & 0 \\ 0 & 0.000205339 \end{bmatrix} \tag{1.61}$$

$$\dot{\tilde{x}}_{\text{int}} = A_{\text{int}}\tilde{x}_{\text{int}} + B_{1,\text{int}}\tilde{u} \tag{1.62}$$

The reachability matrix becomes:

$$\mathcal{R}_{\text{int}} = \begin{bmatrix} B_{1,\text{int}} & A_{\text{int}}B_{1,\text{int}} & A_{\text{int}}^2 B_{1,\text{int}} & A_{\text{int}}^3 B_{1,\text{int}} \end{bmatrix} \tag{1.63}$$

An evaluation of the rank of this matrix using MATLAB's `ctrb` function:

```
R_int = ctrb(A_int, B1_int);
rank(R_int)
```

The resulting rank is 4, which confirms that the internal subsystem is fully reachable.

Stabilizability and the Hurwitz Condition According to control theory, if the system is fully reachable, it is possible to design a state feedback control law:

$$\tilde{u} = K_S \tilde{x}_{\text{int}} \tag{1.64}$$

such that the closed-loop matrix:

$$A_{\text{int}} + B_{1,\text{int}} K_S \tag{1.65}$$

is **Hurwitz**, meaning that all of its eigenvalues lie in the left half of the complex plane. This ensures that the closed-loop system is **BIBS stable** (Bounded

Input Bounded State): all state trajectories remain bounded in response to bounded inputs.

In conclusion, while the full model is not entirely reachable due to the presence of exogenous states, the subsystem representing the vehicle dynamics is fully reachable and can be stabilized using linear state feedback.

Integral Action

While the stabilizer matrix K_S ensures the stability of the internal system under feedback control, an integral action is required to eliminate steady-state error in the presence of unknown constant disturbances $\tilde{w}$.

The regulated error $\tilde{e}$ is defined as:

$$\tilde{e} = C_e\tilde{x} + D_{1e}\tilde{u} + D_{2e}\tilde{w} \tag{1.66}$$

To implement integral control, new integral state η is introduced:

$$\dot{\eta} = \tilde{e} \tag{1.67}$$

This leads to an extended state vector:

$$x_e = \begin{bmatrix} \tilde{x} \\ \eta \end{bmatrix} \tag{1.68}$$

The extended system dynamics are:

$$\dot{x}_e = \bar{A}x_e + \bar{B}_1\tilde{u} + \bar{B}_2\tilde{w} \tag{1.69}$$

where

$$\bar{A} = \begin{bmatrix} A & 0 \\ C_e & 0 \end{bmatrix}, \quad \bar{B}_1 = \begin{bmatrix} B_1 \\ D_{1e} \end{bmatrix}, \quad \bar{B}_2 = \begin{bmatrix} B_2 \\ D_{2e} \end{bmatrix} \tag{1.70}$$

To verify whether the extended system is controllable (reachable), a reachability matrix is computed as:

$$\mathcal{R}_e = \begin{bmatrix} \bar{B}_1 & \bar{A}\bar{B}_1 & \bar{A}^2\bar{B}_1 & \cdots & \bar{A}^{n+q-1}\bar{B}_1 \end{bmatrix} \tag{1.71}$$

where n is the number of original state variables and q is the number of integrator states. In this model, $n = 4$ (excluding the four uncontrollable states) and $q = 2$, so we expect:

$$\text{rank}(\mathcal{R}_e) = 6 \tag{1.72}$$

The reachability matrix is constructed in MATLAB using:

```
Ae = [A, zeros(6,2); Ce, zeros(2,2)];
B1e = [B1; D1e];
Re = ctrb(Ae, B1e);
rank(Re)
```

Result: The output of the command confirms that $\text{rank}(\mathcal{R}_e) = 6$, i.e., the extended system is fully reachable.

Conclusion: Since the extended system is reachable, it is possible to design a state feedback control law of the form:

$$\tilde{u} = \bar{K}x_e = K_S\tilde{x} + K_I\eta \tag{1.73}$$

such that the closed-loop matrix $\bar{A} + \bar{B}_1\bar{K}$ is Hurwitz. This guarantees asymptotic stability of the augmented system and drives the regulation error $\tilde{e}$ to zero.

Observability

Up to this point, the system state $\tilde{x}$ has been assumed to be known. However, this assumption is often unrealistic, particularly when some state variables are not directly measurable. For this reason, a state observer is required to estimate the internal states based on measurable outputs.

Given that the last four states of $\tilde{x}$ are exogenous and not influenced by the system dynamics, we restrict our observability analysis to the internal dynamics only, i.e., $\tilde{x}_{\text{int}} \in \mathbb{R}^4$.

Let C_{int} be the output matrix corresponding to the internal states. Then, the observability matrix is given by:

$$\mathcal{O} = \begin{bmatrix} C_{\text{int}} \\ C_{\text{int}}A_{\text{int}} \\ C_{\text{int}}A_{\text{int}}^2 \\ C_{\text{int}}A_{\text{int}}^3 \end{bmatrix} \tag{1.74}$$

$$C_{\text{int}} = \begin{bmatrix} 0 & 0 & 9.81 & 0 \\ -55.2995 & -3.68664 & 6.52535 & 0.435023 \\ 0 & 0 & 0 & 1 \\ 1 & 0 & 1.362 & 0 \\ 1 & 0 & -1.598 & 0 \\ 0 & 0 & 0 & 0 \\ 0 & 0 & 0 & 0 \end{bmatrix} \tag{1.75}$$

Using MATLAB, it is computed that:

```
O = obsv(A_int, C_int);
rank(O)
```

If $\text{rank}(\mathcal{O}) = n = 4$, the system is **fully observable**, and it is possible to construct a full-order **Kalman filter** (optimal observer):

$$\dot{\hat{x}}_{\text{int}} = A_{\text{int}}\hat{x}_{\text{int}} + B_{1,\text{int}}\tilde{u} + K_f(y - C_{\text{int}}\hat{x}_{\text{int}}) \tag{1.76}$$

where K_f is the **Kalman gain**, computed to optimally minimize the estimation error covariance under the assumption of white Gaussian process and

measurement noise. The Kalman gain is derived from the steady-state solution of the continuous-time algebraic Riccati equation:

$$A_{\text{int}}P + PA_{\text{int}}^T - PC_{\text{int}}^T R^{-1} C_{\text{int}} P + Q = 0 \tag{1.77}$$

$$K_f = PC_{\text{int}}^T R^{-1} \tag{1.78}$$

Here:

- Q is the covariance matrix of the process noise,
- R is the covariance matrix of the measurement noise,
- P is the steady-state error covariance matrix.

By solving the Riccati equation with appropriately chosen Q and R, the filter gain K_f ensures that the estimation error converges in a statistically optimal sense, even in the presence of measurement and process disturbances.

Conclusion:
The MATLAB analysis confirms that $\text{rank}(\mathcal{O}) = 4$, which equals the number of internal states. Therefore, the pair $(A_{\text{int}}, C_{\text{int}})$ is **fully observable**, and a Kalman filter can be designed. This guarantees that despite partial measurements, the entire internal state vector $\tilde{x}_{\text{int}}$ can be optimally reconstructed for control and estimation purposes.

This observability ensures that despite partial measurements, the entire controllable state can be reconstructed and regulated accordingly.

Chapter 2

Application

2.1 Simulator description

2.2 Vehicle Parameters and Numerical Setup

To evaluate the performance of the proposed active suspension control, a numerical setup representative of a luxury high-end sedan (e.g., a Rolls-Royce Ghost or similar) was implemented. The choice of parameters aims to replicate a "Magic Carpet" ride quality, characterized by low natural frequencies and high isolation from road disturbances.

2.2.1 Mass and Geometry

The vehicle body mass is set to $m = 2550$ kg, reflecting the significant weight of luxury vehicles. A perfectly balanced weight distribution is assumed, with $d_f = d_r = 1.65$ m, resulting in a total wheelbase of $L = 3.3$ m.

The pitch moment of inertia J is not assumed as a point mass but calculated using the radius of gyration k_p. For luxury sedans, k_p typically ranges between 35% and 40% of the wheelbase. In this model, we used:

$$J = m \cdot (0.38 \cdot L)^2 \approx 4016 \text{ kg} \cdot \text{m}^2 \tag{2.1}$$

This high inertia value contributes to a more stable and "slower" pitch response, which is perceived as more comfortable by passengers.

2.2.2 Suspension and Tire Characteristics

The stiffness and damping coefficients are tuned to be relatively soft:

- **Spring Stiffness (k_f, k_r):** Values of $35,000$ N/m and $32,000$ N/m are chosen to maintain a low natural frequency (around 1 Hz), which is the human comfort benchmark.

- **Damping (β_f, β_r):** Set at 4200 N·s/m. In a real active system, this would represent the "base" passive damping upon which the actuators exert additional forces.
- **Unsprung Masses (m_{wf}, m_{wr}):** Fixed at 48 kg per wheel, representing large, high-profile luxury wheels.
- **Tire Stiffness (k_{tf}, k_{tr}):** The value of $270,000$ N/m represents high-profile tires which provide additional filtering of high-frequency road noise.

2.2.3 Anti-Pitch Geometry

The anti-geometry coefficients are chosen to provide a subtle but effective correction without compromising the suspension's ability to absorb bumps:

- **Anti-Dive ($\gamma_f = 0.05$):** A 5% anti-dive geometry reduces front-end dip during braking.
- **Anti-Squat ($\gamma_r = 0.08$):** An 8% anti-squat geometry prevents excessive rear-end compression during acceleration.

Table 2.1: Numerical Parameters for the Luxury Sedan Model.

Symbol	**Description**	**Value**	**Unit**
m	Sprung Mass	2550	kg
J	Pitch Inertia	4016	kg·m^2
d_f, d_r	CG to Axle Distance	1.65	m
k_f, k_r	Suspension Stiffness	35000, 32000	N/m
β_f, β_r	Passive Damping	4200	N·s/m
m_{wf}, m_{wr}	Unsprung Mass	48	kg
k_{tf}, k_{tr}	Tire Stiffness	270000	N/m
h_{cg}	CG Height	0.60	m
γ_f, γ_r	Anti-Dive/Squat Coeff.	0.05, 0.08	-

Chapter 3

Control Design

3.1 Proposed Control Architecture

The control strategy adopted for the Rolls-Royce half-car model is based on a **Multi-Loop Output Feedback** architecture, combining optimal state regulation with stochastic estimation. The overall block diagram of the proposed solution is illustrated in Figure

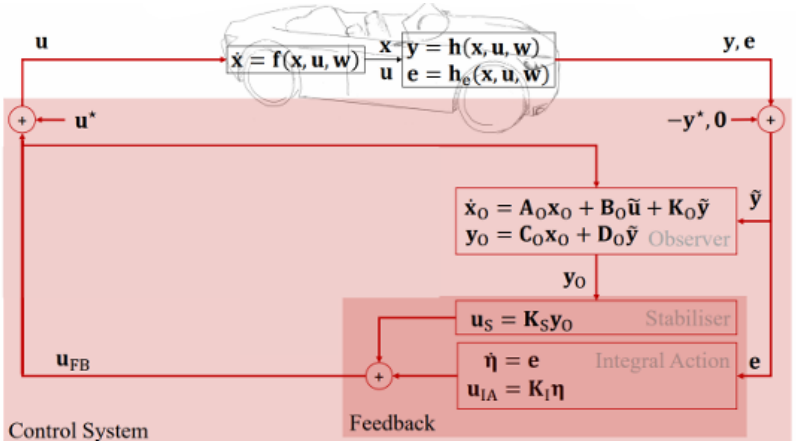

Figure 3.1: Control Architecture

The scheme consists of three main functional blocks:

1. **The Augmented Plant:** Represents the physical vehicle dynamics coupled with the mathematical models of the road disturbances (integrated as stochastic states).

2. **The Kalman Observer:** A state estimator that reconstructs the full state vector $\hat{x}$ (including unmeasurable velocities and road profiles) from

noisy sensor measurements y (suspension deflections and accelerations).

3. **The LQR-Integrator Regulator:** A feedback controller that combines the estimated state $\hat{x}$ for stabilization and damping, and the integral of the error η for set-point tracking.

3.1.1 Design Choice: Implicit Disturbance Rejection vs. Explicit Feed-Forward

A critical design choice in this project was the exclusion of an explicit *Feed-Forward* branch based on "preview" sensors (such as LiDAR or cameras scanning the road ahead). While Preview Control is a common technique in modern active suspensions to prepare the vehicle for upcoming bumps, it was discarded in this architecture for two main reasons:

1. **Hardware Complexity and Cost:** Explicit feed-forward requires additional expensive environmental sensors and high computational power to process road surface data in real-time.

2. **Disturbance Observation Capability:** The designed Kalman Filter is not limited to filtering noise but is configured as a *Disturbance Observer*. By including the road profile states ($z_{road}, \dot{z}_{road}$) in the system model and tuning the process noise covariance matrix (Q_{kal}) aggressively, the observer is capable of estimating the road input virtually instantaneously.

Consequently, the control law $u = -K\hat{x}$ acts on the estimated road states $\hat{\epsilon}$ immediately as the wheel encounters the irregularity. This mechanism creates an **implicit feed-forward action**: the controller "feels" the bump through the unsprung mass dynamics and applies a counter-force before the disturbance propagates significantly to the chassis, achieving the "Magic Carpet" performance without the need for look-ahead sensors.

Le specifiche di progetto includono:

- **Inseguimento del set-point:** Mantenimento dell'altezza statica e dell'assetto orizzontale ($\theta = 0$) anche in presenza di carichi costanti.
- **Reiezione dei disturbi:** Eliminazione dell'errore a regime indotto da irregolarità del manto stradale o forze longitudinali.
- **Dinamica Anti-Pitch:** Compensazione attiva degli effetti di *Anti-Dive* e *Anti-Squat* introdotti dalla geometria delle sospensioni (parametri γ_f, γ_r).

3.2 Architettura di Controllo LQR-PID Aumentata

To ensure the elimination of steady-state error for the controlled variables (heave p_z and pitch θ), the linearized model was extended with two integrator states.

3.2.1 Augmented System and LQR Synthesis

Let $x_{ctrl} \in \mathbb{R}^8$ be the vector of controllable physical states (excluding road kinematics). We define the error vector $e = [e_z, e_\theta]^T$ as the deviation from the reference heights. We introduce the integral state vector $\eta(t) = \int_0^t e(\tau)d\tau$. The augmented system takes the form:

$$\begin{bmatrix} \dot{x}_{ctrl} \\ \dot{\eta} \end{bmatrix} = \begin{bmatrix} A_{ctrl} & 0_{8\times 2} \\ C_{E,ctrl} & 0_{2\times 2} \end{bmatrix} \begin{bmatrix} x_{ctrl} \\ \eta \end{bmatrix} + \begin{bmatrix} B_{ctrl} \\ D_{E1,ctrl} \end{bmatrix} u \tag{3.1}$$

The control gain $K_{aug} = [K_{prop} \quad K_{int}]$ is obtained by minimizing the quadratic cost functional:

$$J = \int_0^\infty (x_{aug}^T Q_{aug} x_{aug} + u^T R_{aug} u)dt \tag{3.2}$$

The weight matrix Q_{aug} was calibrated with a diagonal structure to weigh the proportional, derivative, and integral actions separately:

- **Heave Control:** $q_{pz} = 2 \cdot 10^8$ (P) and $q_{vz} = 8 \cdot 10^5$ (D). The integral action is heavily weighted with $q_{\int z} = 10^{10}$ to force leveling.
- **Pitch Control:** $q_{p\theta} = 3 \cdot 10^9$ (P) and $q_{v\theta} = 10^6$ (D). The integral weight $q_{\int \theta} = 5 \cdot 10^{11}$ is the highest to counteract rotational inertia J and the effects of pitching during braking/acceleration.
- **Unsprung Masses:** $q_{unsprung} = 10^2$, a deliberately low weight to allow the wheels to follow the road profile without transmitting excessive forces to the body.

3.3 State Estimation: Optimal Kalman Filter Theory

Full implementation of the LQR control law requires knowledge of the entire state vector $x \in \mathbb{R}^{12}$. However, in the real system, only a subset of these variables can be measured using sensors (accelerometers and potentiometers). To overcome this, a Kalman filter (KF) has been designed, which acts as an optimal observer in the presence of stochastic noise.

3.3.1 Stochastic Formulation and ϵ Disturbances

The linearized dynamic system is extended to include model and road surface uncertainties, collectively defined as ϵ. The state space model takes the form:

$$\begin{cases} \dot{x} = A_N x + B_1 u + G w \\ y = C_N x + D_1 u + v \end{cases} \tag{3.3}$$

where $w \sim \mathcal{N}(0, Q_{kal})$ represents the process noise (which includes the stochastic variations of the road profile z_{road}) and $v \sim \mathcal{N}(0, R_{kal})$ represents the white noise affecting the sensors.

The states $x_9, \ldots, x_{12}$ (i.e., θ_{road} and z_{road} for the front and rear axles) are not subject to direct control inputs but evolve according to the characteristics of the terrain. The Kalman Filter estimates these "invisible" parameters by analyzing the prediction error on the measurable outputs y.

3.3.2 Observer Dynamics and Innovation

The observer reconstructs the estimated state $\hat{x}$ by minimizing the covariance of the estimation error $P = E[(x - \hat{x})(x - \hat{x})^T]$. The structure of the observer is:

$$\dot{\hat{x}} = A_N \hat{x} + B_1 u + K_o \underbrace{(y - \hat{y})}_{\text{Innovation}} \tag{3.4}$$

The **innovation** term $(y - C_N \hat{x} - D_1 u)$ is the difference between the actual measurement provided by the sensors and the measurement predicted by the model. The gain K_o (calculated in the code using the `lqr` command exploiting duality) determines the weight of the innovation:

- If $Q_{kal} \gg R_{kal}$ (as in the 10^6 vs 10^{-3} setup), the observer considers the model less reliable than the sensors. Consequently, the gain K_o will be high, making the estimation of ϵ extremely fast in following road bumps.
- If $R_{kal} \gg Q_{kal}$, the observer would filter the signals more, but at the risk of "losing" the impulsive component of road disturbances.

3.3.3 Road Profile Reconstruction (Disturbance Observation)

The main advantage of this approach is that the control force u is also calculated as a function of $\hat{\epsilon}$. When a wheel encounters an obstacle, the sudden acceleration of the unsprung mass generates a high innovation in the filter. The latter instantly corrects the estimate of $\hat{z}_{road,f}$ or $\hat{z}_{road,r}$.

The LQR controller, seeing this change in the estimated state, commands the actuators to apply a counterforce even before the disturbance propagates to the main body (sprung mass), effectively performing a sort of **feed-forward (implicit feed-forward)** based on the optimal estimate.

3.3.4 Stability of the Observer

The stability of the estimation is guaranteed by the fact that the pair (A_N, C_N) is observable. In the code, regularization has been applied to the matrix A (`A_reg = A_N - 1e-6*eye(12)`) to prevent numerical instability of the filter during periods of stationarity, ensuring that the eigenvalues of the estimation error $\text{eig}(A_N - K_o C_N)$ have a sufficiently large negative real part to guarantee rapid convergence.

3.4 modeling of Anti-Dive and Anti-Squat Geometry

In a standard half-car model, the suspension struts are often assumed to be perfectly vertical. However, in real vehicle suspension kinematics (e.g., double wishbone or multi-link setups), the instant centers of rotation are designed to create a geometric coupling between longitudinal forces and vertical body forces. This design feature is known as *Anti-Dive* (for the front axle during braking) and *Anti-Squat* (for the rear axle during acceleration).

3.4.1 Geometric Forces Definition

The anti-geometry effects are modeled by introducing two dimensionless coefficients, γ_f and γ_r (represented in the MATLAB code as `gammaf` and `gammar`). These coefficients determine the percentage of the longitudinal force that is converted into a vertical force acting on the sprung mass, bypassing the springs and dampers.

Let $F_{x,f}$ and $F_{x,r}$ be the longitudinal forces at the front and rear tire contact patches respectively (variables `fwfront` and `fwrear`). The vertical forces induced by the suspension geometry, denoted as $F_{v,f}^{geo}$ and $F_{v,r}^{geo}$, are defined as:

$$F_{v,f}^{geo} = \gamma_f \cdot F_{x,f} \tag{3.5}$$

$$F_{v,r}^{geo} = \gamma_r \cdot F_{x,r} \tag{3.6}$$

These forces provide a "stiffening" effect against pitch motion without actually increasing the spring stiffness k_f or k_r, thus preserving ride comfort during steady-state driving while reducing body rotation during aggressive longitudinal maneuvers.

3.4.2 Modified Equations of Motion

The introduction of these geometric forces and the consideration of the center of gravity height (h_{cg}) significantly modify the equilibrium and the dynamics of the sprung mass.

Vertical Dynamics (Heave)

The equation for the vertical acceleration $\ddot{z}$ (variable `f2`) must now account for the geometric lift forces. The Newton's second law for the vertical direction becomes:

$$m\ddot{z} = F_{sf} + F_{sr} + F_{af} + F_{ar} + F_{v,f}^{geo} + F_{v,r}^{geo} - mg \tag{3.7}$$

Where:

- F_{sf}, F_{sr} are the passive suspension forces (spring + damper).

- F_{af}, F_{ar} are the active control forces.
- $F_{v,f}^{geo}, F_{v,r}^{geo}$ are the anti-dive/anti-squat contributions.

Rotational Dynamics (Pitch)

The pitch dynamics are the most affected by these changes. The moment balance equation for $\ddot{\theta}$ (variable `f4`) includes the torque generated by suspension forces, the geometric forces, and the inertial load transfer due to the height of the center of gravity.

The total longitudinal force acting on the vehicle is $F_{tot\_x} = F_{x,f} + F_{x,r}$. This force creates a pitching moment around the center of gravity defined by $M_{long} = F_{tot\_x} \cdot h_{cg}$. The modified rotational equation of motion is:

$$J\ddot{\theta} = d_f \left(F_{sf} + F_{af} + F_{v,f}^{geo} \right) - d_r \left(F_{sr} + F_{ar} + F_{v,r}^{geo} \right) + F_{tot\_x} \cdot h_{cg} \tag{3.8}$$

Here, positive F_x (acceleration) creates a positive pitch moment (nose up), which is counteracted by the Anti-Squat force $F_{v,r}^{geo}$. Conversely, negative F_x (braking) creates a negative pitch moment (nose down), counteracted by the Anti-Dive force $F_{v,f}^{geo}$.

3.4.3 Impact on Linearization

Since the longitudinal forces $F_{x,f}$ and $F_{x,r}$ are treated as external inputs (or disturbances depending on the control architecture), the system matrices B and D in the state-space representation are updated. Specifically, the disturbance matrix regarding longitudinal inputs reflects that a change in throttle or braking now instantaneously affects the vertical acceleration $\ddot{z}$ and pitch acceleration $\ddot{\theta}$ through the γ coefficients and h_{cg}.

3.5 Control Strategy: LQR with Integral Action (LQR-PID)

To achieve precise tracking of the reference height and pitch angle while maintaining passenger comfort, a Linear Quadratic Regulator (LQR) with integral action is implemented. This approach effectively combines the optimal state feedback of LQR with the zero steady-state error property of a PID-type controller.

3.5.1 Augmented System State-Space Representation

In the MATLAB implementation, the control is designed for the controllable part of the system (the 8 physical states of the vehicle body and wheels). To eliminate steady-state offsets in heave (z) and pitch (θ), the state vector is

augmented with two integral states, $e_{int,z}$ and $e_{int,\theta}$, defined as the integral of the error between the measured outputs and the references:

$$x_{aug} = \begin{bmatrix} x_{phys} \\ e_{int} \end{bmatrix} \in \mathbb{R}^{10\times 1}, \quad \text{where } e_{int} = \int (y_{ref} - y)\, dt \tag{3.9}$$

The augmented system matrices, A_{aug} and B_{aug}, are constructed as:

$$A_{aug} = \begin{bmatrix} A_{ctrl} & \mathbf{0}_{8\times 2} \\ C_{E,ctrl} & \mathbf{0}_{2\times 2} \end{bmatrix}, \quad B_{aug} = \begin{bmatrix} B_{ctrl} \\ D_{E1,ctrl} \end{bmatrix} \tag{3.10}$$

where $C_{E,ctrl}$ and $D_{E1,ctrl}$ map the physical states to the tracking errors for heave and pitch.

3.5.2 Optimal Control Law and Tuning

The control law is defined as $u = -K_{aug}x_{aug}$, where K_{aug} is the gain matrix that minimizes the quadratic cost function:

$$J(u) = \int_0^\infty (x_{aug}^T Q_{aug} x_{aug} + u^T R_{aug} u)\, dt \tag{3.11}$$

The tuning is performed through the selection of the diagonal matrices Q_{aug} and R_{aug}. Specifically, the weights in the MATLAB script are organized to balance different performance requirements:

- **Proportional Weights (q_{pz}, q_{ptheta}):** Regulate the reactivity of the system to position errors.
- **Derivative Weights (q_{vz}, q_{vtheta}):** Control the damping of the vertical and angular velocities.
- **Integral Weights ($q_{heave\_int}, q_{pitch\_int}$):** Ensure the elimination of steady-state errors caused by constant disturbances or load changes.

3.5.3 State Estimation: Kalman Filter

Since not all states are directly measurable, a Kalman Filter is designed to estimate the 12 physical states x. The observer gain K_o is calculated by solving the Riccati equation using the process noise covariance Q_{kalman} and the measurement noise covariance R_{kalman}:

$$\dot{\hat{x}} = A_N\hat{x} + B_1 u + K_o(y - C_N\hat{x} - D_1 u) \tag{3.12}$$

The observer allows the controller to use estimated velocities and road states that are otherwise inaccessible via standard sensors.

3.5.4 Linear vs. Non-Linear Implementation

A crucial distinction is made in the final part of the design. While the augmented LQR is designed on the linearized 12-state model $(A_N, B_1, \dots)$, the implementation for the **Non-Linear System** in Simulink uses a reduced 8-state version:

- **Linear Control:** Uses the full K_{prop} (2x12) and K_{int} (2x2) matrices, accounting for road states.
- **Non-Linear Control:** Uses a reduced K_{nonlin_prop} (2x8) which acts only on the physical states of the vehicle, as the road states are treated as external disturbances in the non-linear plant.

3.6 Numerical Control Design Analysis

Based on the theoretical framework established in the previous sections, the numerical synthesis of the control law was performed. The resulting matrices confirm the design choices aimed at achieving superior ride comfort ("Magic Carpet" effect) and robust handling.

3.6.1 Augmented System Dynamics

The augmented state matrix $\mathcal{A}_{aug} \in \mathbb{R}^{10\times 10}$, which includes the integral states for heave and pitch error regulation, is derived as:

Matrix $\mathbf{A_{aug}}$ (scaled by 10^3):

$$\begin{bmatrix} 0 & 1.0 & 0 & 0 & 0 & 0 & 0 & 0 & 0 & 0 \\ -27.5 & -3.3 & 0 & 0 & 13.7 & 1.6 & 13.7 & 1.6 & 0 & 0 \\ 0 & 0 & 0 & 1.0 & 0 & 0 & 0 & 0 & 0 & 0 \\ 0 & 0 & -47.5 & -5.7 & 14.4 & 1.7 & -14.4 & -1.7 & 0 & 0 \\ 0 & 0 & 0 & 0 & 0 & 1.0 & 0 & 0 & 0 & 0 \\ 729.2 & 87.5 & 1203.1 & 144.4 & -6354.2 & -87.5 & 0 & 0 & 0 & 0 \\ 0 & 0 & 0 & 0 & 0 & 0 & 0 & 1.0 & 0 & 0 \\ 729.2 & 87.5 & -1203.1 & -144.4 & 0 & 0 & -6354.2 & -87.5 & 0 & 0 \\ 1.0 & 0 & 0 & 0 & -0.5 & 0 & -0.5 & 0 & 0 & 0 \\ 0 & 0 & 1.0 & 0 & 0 & 0 & 0 & 0 & 0 & 0 \end{bmatrix} \tag{3.13}$$

The last two rows of $\mathcal{A}_{aug}$ (indices 9 and 10) correspond to the integral action dynamics. The terms 1.0×10^{-3} (scaled by 10^3 to unity) represent the integration of the vertical position error e_z and pitch error e_θ, ensuring zero steady-state error.

The input matrix $\mathcal{B}_{aug} \in \mathbb{R}^{10\times 2}$ reflects the direct influence of the control inputs u_1 (heave force) and u_2 (pitch moment) on the vertical velocity (state 2) and pitch rate (state 4), as well as on the unsprung mass dynamics. **Matrix**

$\mathbf{B_{aug}}$:

$$\begin{bmatrix} 0 & 0 \\ 0.0004 & 0 \\ 0 & 0 \\ 0 & 0.0002 \\ 0 & 0 \\ -0.0104 & -0.0063 \\ 0 & 0 \\ -0.0104 & 0.0063 \\ 0 & 0 \\ 0 & 0 \end{bmatrix} \tag{3.14}$$

3.6.2 Optimal LQR Gains Analysis

The control law $u(t) = -K_{prop}\hat{x}(t) - K_{int}\eta(t)$ is characterized by the computed gain matrices.

Proportional-Derivative Action (K_{prop})

The proportional and derivative gains for the physical states are given by:

$$K_{prop} = 10^4 \cdot \begin{bmatrix} 1.67 & 0.54 & 0 & 0 & -0.80 & 0.001 & -0.80 & 0.001 \\ 0 & 0 & 8.93 & 1.52 & -2.28 & 0.004 & 2.28 & -0.004 \end{bmatrix} \tag{3.15}$$

Analysis of these values highlights the control strategy:

- **Pitch Priority:** The gain on the pitch angle ($8.93 \cdot 10^4$) is significantly larger than the gain on vertical displacement ($1.67 \cdot 10^4$). This reflects the design intent to heavily suppress pitch motions, which are critical for passenger comfort in a luxury vehicle.
- **Active Damping:** The derivative gains (columns 2 and 4: $0.54 \cdot 10^4$ and $1.52 \cdot 10^4$) provide substantial active damping, replacing passive dissipation to quickly attenuate oscillations.
- **Sky-Hook Approximation:** The gains on unsprung mass velocities (columns 6 and 8) are negligible (≈ 0), indicating a control strategy that approximates a "Sky-Hook" damper, isolating the body from high-frequency wheel motions.

Integral Action (K_{int})

The integral gains are:

$$K_{int} = 10^5 \cdot \begin{bmatrix} 0.22 & 0 \\ 0 & 1.58 \end{bmatrix} \tag{3.16}$$

The integral gain for pitch ($1.58 \cdot 10^5$) is roughly an order of magnitude higher than for heave ($0.22 \cdot 10^5$). This aggressive integral action on pitch ensures rapid correction of static attitude changes during acceleration or braking (anti-squat/anti-dive compensation).

3.6.3 State Estimation and Road Profile Reconstruction

The full-order Kalman Observer gain matrix $K_o \in \mathbb{R}^{12\times 5}$ (reported in the Appendix) demonstrates the observer's bandwidth. Notably, the gains associated with the road profile states (rows 9-12 of K_o) exhibit values up to $2.0 \cdot 10^4$. This high sensitivity to sensor innovations ($y - \hat{y}$) confirms that the observer is tuned to rapidly estimate road irregularities ("epsilon" states), effectively distinguishing them from sensor noise. This allows the controller to react to road bumps almost instantaneously, approximating a feed-forward response.

Full Kalman Gain $\mathbf{K_o}$ (10^5):

$$\begin{bmatrix} -0.00 & -0.32 & -0.00 & -0.16 & -0.16 \\ -0.00 & -0.07 & -0.00 & -0.22 & -0.22 \\ 0.31 & -0.00 & 0.00 & 0.05 & -0.05 \\ 0.00 & 0.00 & 0.32 & -0.00 & 0.00 \\ 0.05 & 0.06 & 0.00 & -0.37 & -0.07 \\ 0.71 & 0.03 & 8.31 & -2.12 & 2.51 \\ -0.05 & 0.06 & -0.00 & -0.07 & -0.37 \\ -0.71 & 0.03 & -8.31 & 2.51 & -2.12 \\ -0.00 & 0.00 & 0.00 & 0.00 & -0.00 \\ 0.00 & -0.00 & -0.00 & -0.00 & 0.00 \\ 0.02 & 0.00 & 0.21 & -0.06 & 0.06 \\ -0.02 & 0.00 & -0.21 & 0.06 & -0.06 \end{bmatrix} \tag{3.17}$$

3.7 Metriche di Performance

Per quantificare l'efficacia del sistema "Magic Carpet Ride", vengono analizzati i seguenti parametri:

- **Comfort (Body Acceleration):** Analisi dei picchi di accelerazione verticale $\ddot{p}_z$ e angolare $\ddot{\theta}$. Un sistema efficace deve ridurre questi picchi del 30-50% rispetto alla configurazione passiva.
- **Working Space:** Verifica che l'escursione della sospensione s_1 e s_3 non superi i limiti meccanici (tipicamente ± 0.1 m).
- **Handling (Tyre Load):** Monitoraggio delle forze verticali sugli pneumatici (f_{tf}, f_{tr}) per garantire che la ruota non perda mai il contatto con il suolo (condizione $f_t > 0$).

- **Precisione della stima:** Confronto tra i disturbi stradali reali z_{road} e gli "epsilon" stimati $\hat{z}_{road}$ dal filtro di Kalman.

3.8 Analisi Risultati (Risultati Attesi)

Sulla base del tuning effettuato nel Control Design, si prevedono i seguenti comportamenti nelle simulazioni:

3.8.1 Risposta al Bump

Ci si aspetta che l'azione attiva degli attuatori f_{af} e f_{ar} intervenga immediatamente al rilevamento del dosso tramite l'osservatore. L'integrazione dell'errore dovrebbe permettere alla vettura di tornare all'altezza nominale ℓ_0 senza oscillazioni residue significative (*deadbeat-like response*), grazie all'elevato peso q_{int} assegnato agli stati integrali.

3.8.2 Effetto Anti-Dive e Anti-Squat

Durante le fasi di accelerazione e frenata (simulate tramite F_{wfront} e F_{wrear}), il sistema di controllo deve compensare il momento di beccheggio indotto dall'altezza del baricentro h_{cg}. Ci si aspetta che l'angolo di pitch θ rimanga prossimo allo zero, dimostrando l'efficacia della geometria attiva del modello rispetto a una sospensione passiva tradizionale.

3.8.3 Robustezza al Rumore

L'introduzione dei rumori di misura (`nuy, nuz, nug, nuf, nur` nel codice) metterà alla prova il filtro di Kalman. La performance sarà considerata soddisfacente se la stima degli stati $\hat{x}$ rimarrà stabile e se il controllo non presenterà un *chattering* eccessivo sugli attuatori.

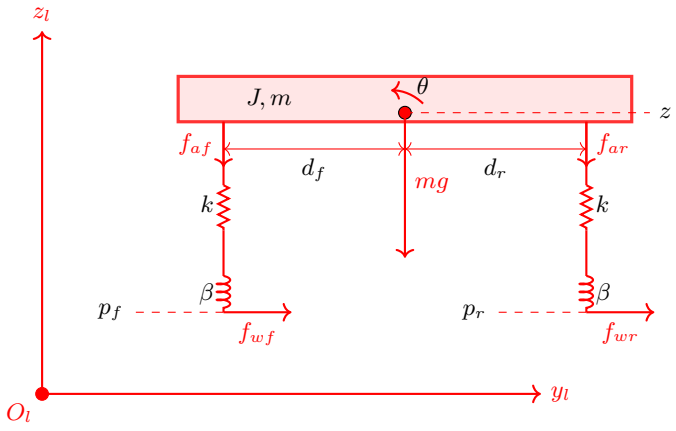

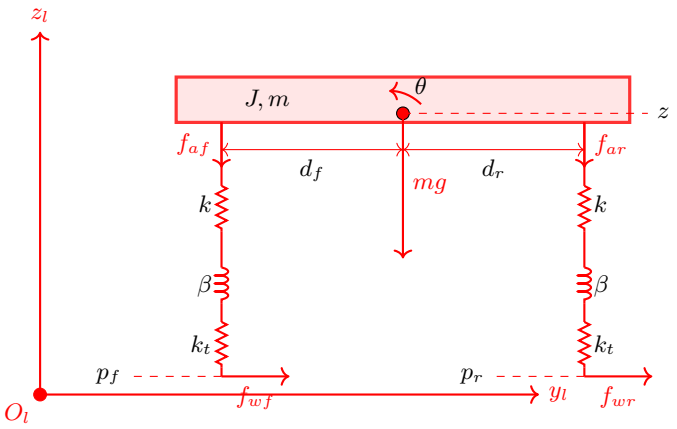

todo: finire sto disegno

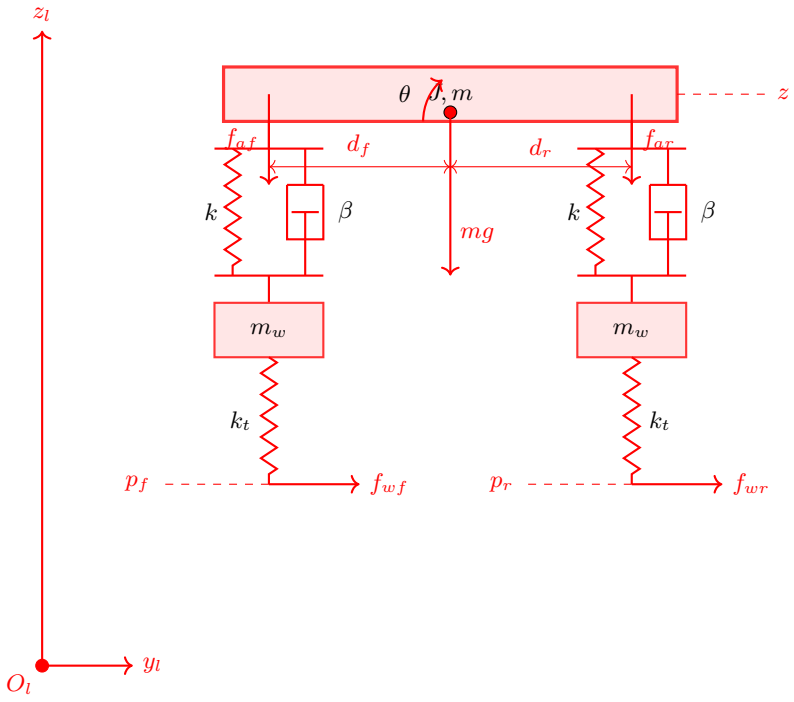

Copy and past the Simulink block scheme and describe what each block does. Describe the set-up MATLAB file, where and how to change the parameters of the simulations. Remember to include also the sensor noises and realistic external disturbances.

3.9 Simulation results

Describe the simulation scenario: initial conditions, purpose of the simulation. Describe the results: are the results coherent with the expectation? If not why? Investigate the tuning: how the performance are affected by the selection of the parameters at disposal of the designer?

Chapter 4

Conclusions and further investigation

Recap the main results obtained in the project and highlight eventual further investigation directions alogn which the performance could be improved.

Bibliography

List the papers/books cited.

Appendix

Use appendices to add technical parts which are instrumental for the completeness of the manuscript but are too heavy to be included inside the main text. Basically, appendices are exploited to let the main text cleaner and smoother. As example, the complete MATLAB listings can be reported in appendix.